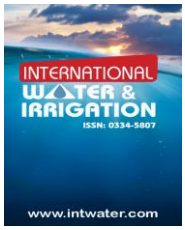

International Water and Irrigation
ISSN: 0334-5807
Volume 44 Issue 2, (2025)
Pages 583-600

Eutrophication Inversion of Reservoir Waters Based on Deep Learning and UAV Hyperspectral Remote Sensing

Fenghua Huang [1,2,*], Zhenyu Zhu [1,2], Bingzheng Li[1,2,3], Yansong Liao[1,2,3], Zhen Zheng[4], Jihui Liu[5]

[1]Fujian Key Laboratory of spatial information perception and intelligent processing (Yango University), 350015 Fuzhou, China; fhhuang@ygu.edu.cn (F.H.)

[2]Fujian University Engineering Research Center of Spatial Data Mining and Application (Yango University) , 350015 Fuzhou, China; zxiaoyu2303@163.com (Z.Y.Z.)

[3]Academy of Digital China (Fujian), Fuzhou University, Fuzhou 350108, China; libingzheng2021@163.com (B.L.) ;225527022@fzu.edu.cn (Y.L.)

[4]Fuzhou Academy of Environmental Sciences, Fuzhou 350000, China; zzme110@126.com (Z.Z.);

[5]Fujian Academy of Environmental Sciences, Fuzhou 350013, China; LiuJH0323@126.com (J.L.)

*Correspondence: fhhuang@ygu.edu.cn

Abstract: Eutrophication of reservoir water poses significant risks to human life and production, necessitating large-scale, regular monitoring and early warning. This work comprehensively evaluated the eutrophication status of reservoir water quality using four water quality parameters: chlorophyll a (Chl-a), Total Phosphorus (TP), Total Nitrogen (TN) and Permanganate Index (COD_{Mn}). A water quality parameter inversion scheme based on deep learning and UAV hyperspectral remote sensing images is proposed. Based on the optimized feature combinations and sample sets, a water quality parameter concentration regression prediction model based on deep convolutional residual neural network (WQR-DCRNN) is designed and constructed for the inversion of the water quality parameters of Chl-a, TP, TN, and COD_{Mn}. Then, the parameters of above WQR-DCRNN models are optimized by reinforcement learning. Taking Shanzai Reservoir in Fuzhou City as an example, the average inversion accuracy of the four water quality parameters reached 0.91, 0.80, 0.81, and 0.78, respectively, and the mean relative error (MRE) can meet the requirement of the industrial standards for spectral water quality detection. The concentration spatial distribution patterns of the four water quality parameters provided by this work can provide useful decision-making references for the assessment, prevention and control of eutrophication in large-scale reservoir water bodies.

Keywords: Deep Learning; Reservoir water quality inversion; Hyperspectral remote sensing; Eutrophication monitoring

1. Introduction

Reservoirs are an important component of land ecosystems and one of the main water sources for human production and life. Due to human activities or natural factors, a large amount of nutrients such as nitrogen and phosphorus required by organisms enter slow-moving water bodies such as reservoirs, leading to water quality eutrophication phenomenon [1]. Eutrophication phenomenon(such as "algal blooms") have significant harm, which can easily lead to the proliferation of algae and other planktonic organisms in reservoirs, a decrease in dissolved oxygen content, massive death of fishes and other organisms, and discoloration of water bodies. The current eutrophication of water bodies, such as "algal blooms," has become a major challenge for global ecology of lakes and reservoirs and drinking water safety. It is crucial to regularly carry out large-scale, high-precision, and high-efficiency monitoring of reservoir water quality to timely control the trend of changes in reservoir water quality [2]. However, traditional water quality monitoring methods (such as biological and chemical methods) face many challenges for monitoring the eutrophication status of large-scale lake and reservoir water bodies, including high cost, time-consuming, and can only detect water quality conditions at discrete points, which cannot

International Water and Irrigation
ISSN: 0334-5807
Volume 44 Issue 2, (2025)
Pages 583-600

provide spatial distribution of water quality in large-scale water bodies[3-5]. The water quality inversion technology based on remote sensing can establish a fitting relationship model between the concentration of water quality parameters and the related spectral reflectance characteristic curve at sampling points through commonly used regression algorithms in traditional machine learning methods, achieving large-scale reservoir water quality parameter inversion [6-7]. However, traditional multispectral satellite images have relatively less bands and lower resolution, and traditional regression models are difficult to solve complex nonlinear fitting problems, which greatly limits the accuracy of remote sensing water quality inversion [8-12]. Hyperspectral remote sensing images often have hundreds or thousands of continuous bands, especially airborne hyperspectral technology can capture richer spectral and texture information, which can more accurately identify subtle changes in surface features [13-15]. In addition, recently related researches have shown that deep learning methods have demonstrated unique advantages in water quality inversion and spectral information reconstruction. Deep learning frameworks such as Convolutional Neural Networks (CNN), Long Short Term Memory (LSTM), and Sequence to Sequence (Seq2Seq) have been successfully used to solve regression prediction problems based on hyperspectral remote sensing images, with high accuracy and stability [16-17]. Obviously, the combination of deep learning regression algorithms and airborne hyperspectral data can establish high-accuracy models for concentration estimation of water quality parameters, effectively improve the accuracy of remote sensing inversion of surface water quality and more accurately predict the spatial distribution of inland water eutrophication, which is conducive to early detection and tracing source analysis of eutrophication for lake and reservoir waters.

In order to solve the above problems, this work intends to introduce a water quality parameter regression prediction model based on deep convolutional residual neural network (WQR-DCRNN) and unmanned aerial vehicle (UAV) hyperspectral remote sensing technology. Combining the measured spectral information and water quality parameters concentration of the samples from Shanzai Reservoir in Fuzhou city, the inversion models of different water quality parameters are constructed to perform remote sensing inversion of the four corresponding water quality parameters(chlorophyll a (Chl-a), total phosphorus (TP), total nitrogen (TN), and Permanganate Index (COD_{Mn})) in the reservoir, in order to achieve large-scale dynamic monitoring of the eutrophication status of Shanzai Reservoir water quality. This work can provide more comprehensive decision support information for urban water source management, improve the accuracy and practicality of remote sensing inversion of reservoir water quality, and provide useful references for the prevention and control of eutrophication in reservoir water bodies.

2. Materials and Methods

1.1. Experimental area and of samples distribution

This project takes Shanzai Reservoir (in Lianjiang County, Fuzhou City, Fujian Province, China) as an example for research. Shanzai Reservoir is a medium to large reservoir (valley type) constructed through dam construction, with a total surface area of 3.5 square kilometers. Shanzai Reservoir was designated as the second drinking water source in Fuzhou City in 1997, with water supply areas including surrounding Jin'an District, Lianjiang County, and Luoyuan County, which had a significant impact on the production and daily life of residents in the surrounding districts and counties. However, due to the disorderly discharge of industrial and agricultural production and domestic sewage in the surrounding areas, some water bodies of the above-mentioned reservoir have shown significant eutrophication in recent years, resulting in the concentration of some water quality parameters (such as chlorophyll, algae count, total nitrogen, total phosphorus, etc.) exceeding the relevant water environment quality standard, which has a certain impact on the ecological balance as well as production and living water safety of the surrounding areas. Therefore, it is imperative to regularly carry out large-scale, high-accuracy, and high-efficiency water quality monitoring and timely grasp the water quality changes in reservoirs. The experimental area and samples distribution of Shanzai Reservoir are shown in Figure 1.

International Water and Irrigation
ISSN: 0334-5807
Volume 44 Issue 2, (2025)
Pages 583-600

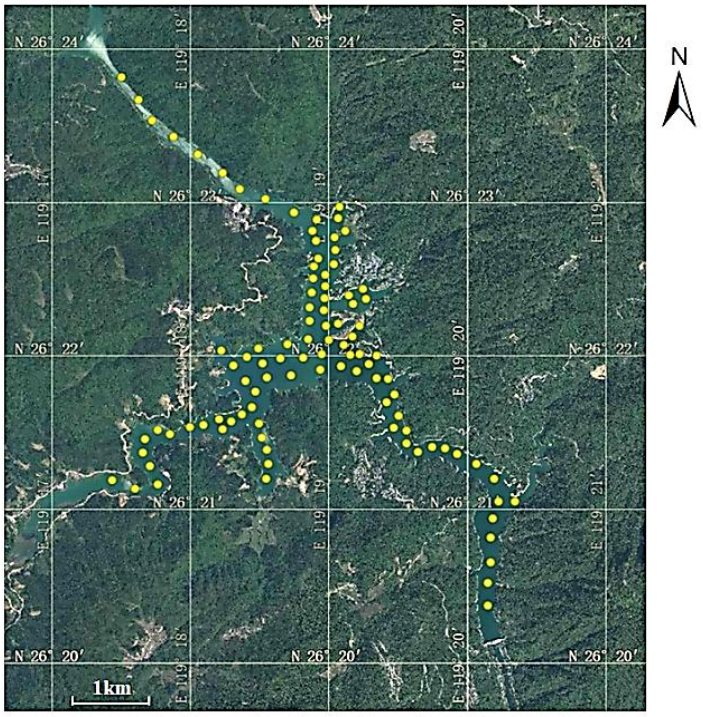

Figure 1 Experimental area and samples distribution of Shanzai Reservoir(highlighted by yellow dots).

1.2 Water samples collection and spectrum detection

This work collected water samples and corresponding spectral information from Shanzai Reservoir in four different times, such as on December 3, 2021 (winter), March 16, 2022 (spring), June 13, 2022 (summer), and September 26, 2022 (autumn). 100 water samples were collected each time at the same sampling locations respectively, and after removing invalid samples, 95, 93, 95, and 92 valid water samples were obtained in each of the four collections. A time period with abundant sunlight was selected, and a standard sampler with a capacity of one liter was used to collect water samples at each sampling point fifty centimeters underwater, meanwhile the locations of the sampling points were accurately recorded by a real-time kinematic (RTK) equipment. Simultaneously, an UAV equipped with a hyperspectral camera (device model: GaiaSky-mini) was used to capture images of the surrounding water surface near the sampling point in a suspended state (Number of bands: 360, flight height: 150meters, image resolution: about 30 centimeters, spectral wavelength range: 400~1000nm), ensuring the synchronization of spectral detection and water sample collection. Then the hyperspectral images of the collected water samples were preprocessed (including lens correction, reflectance correction and atmospheric correction, et al.), and the average spectral reflectance value of all pixels in the 3 × 3 neighborhood window centered on the sampling point was taken as the spectral feature value at the sampling point. Finally, the water samples were sent to a qualified water quality testing institution laboratory for testing to ensure the accuracy of the water quality parameter values. In principle, the near surface spectral curves of all water sampling points mentioned above should have similar waveform characteristics, so the abnormal curves with significant deviations were removed.

International Water and Irrigation
ISSN: 0334-5807
Volume 44 Issue 2, (2025)
Pages 583-600

1.3 Acquisition and stitching of hyperspectral images of water bodies to be inverted

The same UAV-carried hyperspectral camera mentioned above was used to continuously capture images of the water area to be inverted according to the pre-designed route. The flight altitude was also about 150 meters, and the overlap ratio of lateral and route is set to 40%. The collected hyperspectral image data has 360 bands with a spectral range of 400-1000nm. After the capture was completed, all relevant images were exported from the hyperspectral camera and preprocessed by the same method mentioned above. Finally, the preprocessed images were automatically mosaicked to generate a whole hyperspectral image of the water area to be inverted. The whole mosaicked hyperspectral image of the water bodies to be inversed (taking the data collected on December 3, 2022 as an example) are shown in Figure 2.

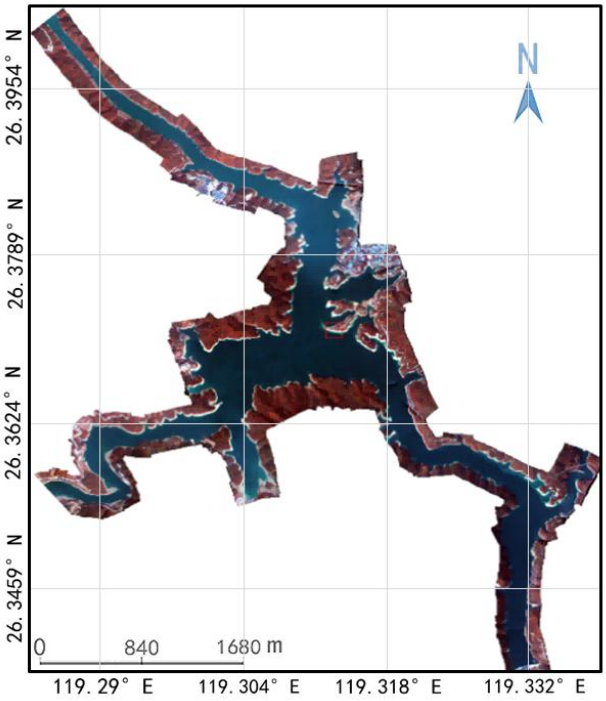

Figure 2. The whole mosaicked hyperspectral image of the water bodies to be inversed (2022-12-03).

1.4 Sample augmentation

Sample data augmentation technology involves a series of processing and transformations on the original sample set to expand more simulated training samples, so as to compensate for the insufficient number of training samples, and thus improve the accuracy and generalization ability of the final model. Due to the high cost of water sample collection and analysis, as well as the difficulty of collecting water surface spectral information, the amount of labeled sample data is often limited in actual water quality prediction modeling, which contradicts the requirement of relying on a large number of labeled samples for deep learning model construction. In this work, the feature space of the original training sample set is a high-dimensional space (361 feature dimensions in total) composed of the measured concentration values of one of the four water quality parameters and the corresponding near surface spectral reflectance information (360 bands). The UAV hyperspectral images corresponding to each sampling point were rotated by 90 degrees, 180 degrees, and 270 degrees, respectively, so that each sampling point was corresponded to four hyperspectral images from different angles. The original training sample set was augmented to improve the accuracy of water quality parameter regression prediction. Through the above opera-

International Water and Irrigation
ISSN: 0334-5807
Volume 44 Issue 2, (2025)
Pages 583-600

tions, the sample size was increased to 1500, which could better meet the needs of model training, testing, and evaluation. This processing method can not only fully utilize the collected data, but also improve the robustness and generalization ability of the model, thereby better achieving the research objectives.

1.5 Feature Dimensionality Reduction and Correlation Analysis

Hyperspectral images typically have hundreds to thousands of continuous bands and possess strong ground recognition capabilities. However, due to issues such as high feature dimensionality and high redundancy, overfitting is prone to occur, especially when the sample size is small. Proper dimensionality reduction while preserving the main features of hyperspectral images can effectively improve the efficiency of model construction. Therefore, this work adopted the following band filtering algorithm for feature dimensionality reduction, in order to reduce data complexity and improve data quality.

1. Successive Projection Algorithm (SPA): It is an effective feature selection method that can obtain efficient feature bands in a short period of time, remove redundant spectral information from the original spectrum, or find the variable combination with the least redundant information from the spectral variables, and maximize the acquisition of data interpretation information, so as to reduce model complexity. SPA has a wide range of applications in hyperspectral remote sensing research in fields such as agriculture and ecological environment.

2. Pearson Correlation Analysis Method (PCAM): It is mainly used to reflect the degree of correlation between two feature variables, that is, to measure the linear correlation between spectral features and water quality parameters. This work mainly used PCAM to select band combinations which were suitable for the inversion of various water quality parameters. The calculation method of the correlation coefficient (r_{xy}) is as formula (1):

$$r_{xy} = \frac{\sum_{i=1}^{n} (x_i - \bar{x})(y_i - \bar{y})}{\sqrt{\sum_{i=1}^{n} (x_i - \bar{x})^2}\sqrt{\sum_{i=1}^{n} (y_i - \bar{y})^2}} \quad (1)$$

In the formula (1), r_{xy} represents the correlation coefficient between x and y (measuring the linear relationship between the two variables x and y). x_i and y_i respectively represent the *i-th* observed values of the two variables, and $\bar{x}$ and $\bar{y}$ respectively represent the averages of all observed values of the two variables. The range of correlation coefficients r_{xy} is from -1 to 1, where a value of 1 indicates the strongest positive correlation, a value of -1 indicates the strongest negative correlation, and a value of 0 indicates no correlation. The commonly used dual band combination methods include: difference index (DI), ratio index (RI) and normalized difference index (NDI), and their calculation methods are as formula (2), formula (3) and formula (4):

$$DI(B_i, B_j) = B_i - B_j \quad (2)$$

$$RI(B_i, B_j) = \frac{B_i}{B_j} \quad (3)$$

$$NDI(B_i, B_j) = \frac{B_i - B_j}{B_i + B_j} \quad (4)$$

In the formulas (2), (3) and (4), i and j are integers with values ranging from 1 to 360. B_i and B_j represent the values of hyperspectral band i and band j.

International Water and Irrigation
ISSN: 0334-5807
Volume 44 Issue 2, (2025)
Pages 583-600

To avoid multicollinearity, the variance inflation factor (*VIF*) algorithm was introduced to further analyze the selected band combinations. When the value of *VIF* is greater than 10, it indicates that the multicollinearity of the band combination is strong and the corresponding band or band combination needs to be discarded. The calculation method of *VIF* is as formula (5):

$$VIF = \frac{1}{(1 - R^2)} \qquad (5)$$

In the formula (5), *R* is the correlation coefficient between the relevant factors.

1.6 Water Quality Parameter Regression Model Based on Deep Convolutional Residual Neural Network (WQR-DCRNN)

As water quality monitoring is a long-term process that requires periodic water quality sampling and detection, the WQR-DCRNN model not only needs to have high estimating accuracy of water quality parameters, but also needs to have incremental learning capabilities to avoid repetitive training on old sample sets. Traditional estimation models of water quality parameters generally have wearer incremental learning capabilities and rely solely on spectral information for regression learning, ignoring other information such as spatial texture and color, which limits regression accuracy and scalability. This work proposes a water quality parameter regression model based on deep convolutional residual neural network (WQR-DCRNN), which introduces residual blocks and attention modules, and comprehensively considers the spectral features of water samples and the spatial features around sampling points to improve the accuracy and incremental learning performance of the WQR-DCRNN model.

WQR-DCRNN mainly consists of three convolutional block attention modules (CBAM), three residual blocks, four batch normalization layers, four ReLu activation function modules, one dropout layer, four hidden layers and two fully connected layers. The model structure and implementation process of WQR-DCRNN are shown in Figure 3. As shown in Figure 3, in WQR-DCRNN, there is one convolutional attention block, one batch normalization layer, and one ReLu activation function module between each hidden layer. Additionally, there is one residual block before hidden layer 1, hidden layer2 and hidden layer3 respectively. CBAM is an attention mechanism module composed of two components: channel attention module and spatial attention module. Through these two modules above, adaptive feature selection and enhancement are performed on the input feature map in both the channel and spatial directions respectively, highlighting the main features and suppressing irrelevant ones. This enables the WQR-DCRNN network to focus more on the content and location information of the target to be detected, thereby improving the learning accuracy of the WQR-DCRNN network. The main function of the residual blocks is to prevent gradient vanishing and Gradient explosion phenomenon caused by too many hidden layers. The Relu function, with its linear and unsaturated characteristics, can overcome the problem of gradient vanishing to a certain extent and accelerate training speed. The batch normalization module is mainly used to normalize the input and output data of each layer. After multiple rounds of training on a deep neural network consisting of multiple residual blocks, convolutional attention modules, and hidden layers, representative features are outputted to the fully connected layer. Two fully connected layers are responsible for generating the regression model and outputting the regression results.

International Water and Irrigation
ISSN: 0334-5807
Volume 44 Issue 2, (2025)
Pages 583-600

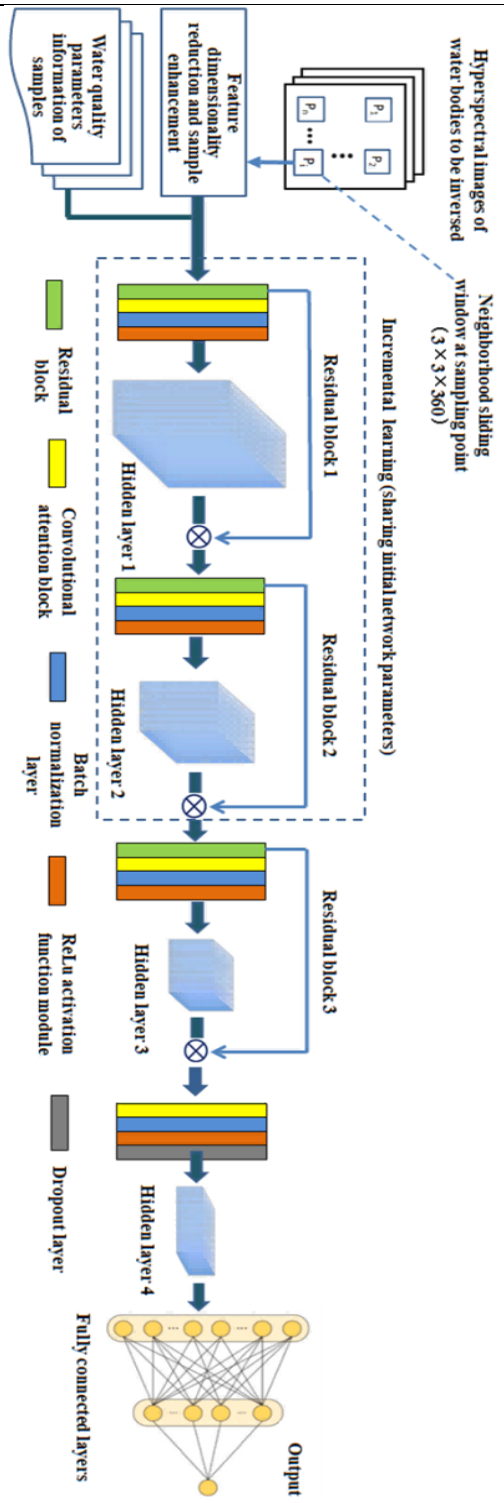

Figure 3. Implementation process of WQR-DCRNN.

In the learning of WQR-DCRNN, due to the comprehensive consideration of spectral and spatial features, the neighborhood window centered on water quality sampling points in a hyperspectral image with 360 bands is a three-dimensional data block (3×3×360). After feature dimensionality reduction, the feature bands of the data

International Water and Irrigation
ISSN: 0334-5807
Volume 44 Issue 2, (2025)
Pages 583-600

blocks will be compressed into a reasonable interval, and the number of data blocks will increase threefold after sample augmentation. The three-dimensional data block, which has undergone feature dimensionality reduction and sample augmentation, is combined with four water quality parameters information to form the final sample set for WQR-DCRNN learning in this work (with training and testing samples accounting for 70% and 30%, respectively).

Many related researches [16-17] have shown that in incremental learning or transfer learning of multi-layer neural network models, the hidden layers near the input layer usually focuses more on learning the underlying common features of the training samples. After learning from the same or similar training sample sets, almost identical network structures can be formed. This work intends to adopt a fine-tuning strategy for incremental learning of WQR-DRCNN. After importing newly labeled samples, the entire regression model will not be retrained from origin. Instead, the shared network parameters of the first to second hidden layers in the previous round of regression models are directly used as the starting parameters for the new model, and only the third hidden layer is used for new training. This greatly improves the efficiency of incremental learning while basically maintaining accuracy.

In this work, reinforcement learning techniques were used to optimize the WQR-DCRNN model, embedding the optimization process of WQR-DCRNN into the framework of reinforcement learning. Through multiple iterations, the optimal parameters of the model were obtained.

1.7 Model Evaluation

This work used statistical relevant indexes to evaluate the model, mainly including coefficient of determination (R^2), root mean square error (*RMSE*), and mean relative error (*MRE*). R^2 is an important index for evaluating the goodness of fit of a model, and the closer its value is to 1, the better the predictive performance of the model. *MRE* is an index used to evaluate the performance of prediction models, typically used to evaluate the accuracy of regression models, representing the average relative error between model predictions and real observations. *RMSE* is used to measure the error between estimated values and true values, with smaller values indicating better fitting performance. The calculation methods of the indexes above are shown as formula (6), (7) and (8).

$$R^2 = 1 - \frac{\sum_{i=1}^{n} \left(t_i - p_i\right)^2}{\sum_{i=1}^{n} \left(t_i - \bar{t}\right)} \quad (6)$$

$$MRE = \frac{1}{n}\sum_{i=1}^{n} \left|\frac{t_i - p_i}{t_i}\right| \quad (7)$$

$$RMSE = \sqrt{\frac{\sum_{i=1}^{n} (p_i - t_i)^2}{n}} \quad (8)$$

In the formulas (6),(7)and (8), p_i and t_i are the predicted and true concentration values of a water quality parameter at the *i-th* water sample point respectively, $\bar{t}$ is the average true concentration values of a water quality parameter of all water samples, and *n* is the total number of water samples.

3. Results

3.1 Spectral feature dimensionality reduction and feature variable combination

In this work, among the four water quality parameters to be inverted, Chl-a is a water quality parameter with obvious spectral response, while TP, TN, and COD_{Mn} are water quality parameters with weaker spectral response. As for Chl-a inversion, firstly, SPA and PCAM are used to filter sensitive bands or band combinations respectively, and then the band combinations selected by the above two methods are directly used as feature variable

International Water and Irrigation
ISSN: 0334-5807
Volume 44 Issue 2, (2025)
Pages 583-600

combinations; For the inversion of water quality parameters with weaker spectral response, additional water quality parameters with obvious spectral response (such as total suspended solids concentration (TSS)) with high correlation with them need to be added to improve the combination of feature variables.

Taking the construction of feature vector for the Chl-a concentration prediction model learning of Shanzi Reservoir on June 13, 2022 as an example, the SPA method was firstly used to filter the original bands, obtaining six representative bands (center wavelengths: 474nm, 529nm, 689nm, 671nm, 711nm, and 943nm); Secondly, all chlorophyll-a reflectivity spectral bands were traversed and PCAM was performed, and the values of the three indexes (DI, RI and NDI) corresponding to any dual-band combinations were calculated. The top five dual-band index values with the highest Pearson coefficients were selected as feature variables for model training, including three DI index values: DI(606,505),DI(699,682), DI(706,465), 1 RI index value: RI(701,472),and 1 NDI index value: NDI(528,524), as shown in Figure 4. Then, VIF method was used to filter the five dual-band indexes mentioned above, and two dual-band indexes that met the requirements were: DI (606,505) and NDI (528,524). The final selected feature combination for chlorophyll-a inversion is a combination of 6 bands filtered by SPA and 2 dual-band indexes filtered by PCAM+VIF.

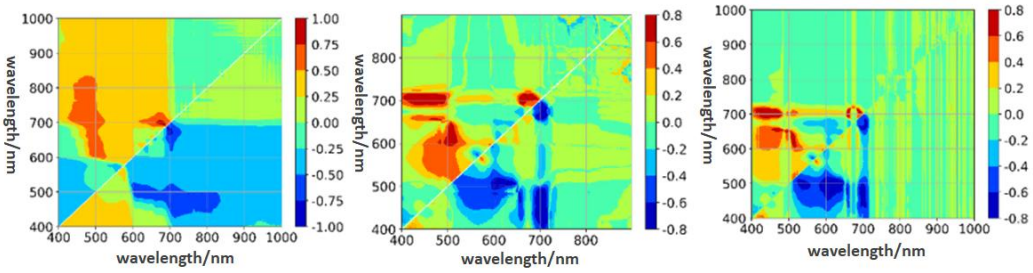

(a) (b) (c)

Figure 4. The heat maps of the correlation between chlorophyll-a concentration and dual-band indexes for (a) DI, (b) NDI and (c) RI.

Due to the insensitivity of spectral responses to the changes of TP, TN, and COD_{Mn} concentrations, when the final modeling feature vector is built, additional features from other water quality parameters with obvious spectral response and high correlation need to be added to improve their inversion accuracy. Taking the construction of feature vector for the TN concentration prediction model learning of Shanzai Reservoir on June 13, 2022 as an example, firstly, by calculating the correlation coefficients between all water quality parameters, it can be concluded that the water quality index with obvious spectral response and the highest correlation with TN in this work is Total Suspended Solids (TSS), with a correlation coefficient of 0.62. Then, six representative bands which responded obviously to the changes of TN concentration, with the center wavelengths of 532nm, 668nm, 846nm, 886nm, 996nm and 943nm, were selected by SPA, and the PCAM dual-band index selection results for concentration prediction model learning of TN and TSS were respectively DI (584,571) and NDI (598,571) (as shown in Figure 5), as well as DI (662,504) and DI (683,494). Therefore, the feature vector of the TN concentration inversion model learning were a combination of the 6 bands selected for TN by SPA, 2 dual-band indexes selected by PCAM for TN, and 2 dual-band indexes selected by PCAM for TSS.

TP and COD_{Mn} are also the water quality parameters with weaker spectral response. The methods of spectral feature dimensionality reduction and inversion feature variables combination of them are basically the same as that for TN, and so will not be repeated here.

International Water and Irrigation
ISSN: 0334-5807
Volume 44 Issue 2, (2025)
Pages 583-600

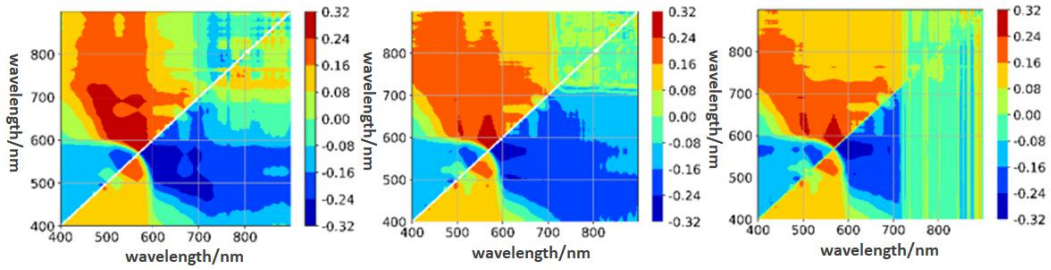

(a) (b) (c)

Figure 5. The heat maps of the correlation between TN concentration and dual-band indexes for (a) DI, (b) NDI and (c) RI.

3.2 WQR-DCRNN model training and inversion result analysis

For any one of the four water quality parameters of Chl-a, TP, TN, and COD_{Mn}, 70% of the samples in the four sample sets (ds1~ds4) collected in four time phases (2021-12-03, 2022-03-16, 2022-06-13 and 2022-09-26) were selected randomly as train samples to train the WQR-DCRNN models respectively ,while the remaining 30% of samples in each sample set were used as the test sets, and four WQR-DCRNN models (wd1~wd4) in different time phases were obtained. Using the wd1~wd4 models above, the concentrations of Chl-a, TP, TN and COD_{Mn} of Shanzai Reservoir waters in Fuzhou City were inverted, and the inversion results are shown in Table 1.

Table 1. Water quality inversion results through WQR-DCRNN in Shanzai Reservoir, Fuzhou City.

Water quality parameter	Evaluation index	2021-12-03 (ds1)	2022-03-16 (ds2)	2022-06-13 (ds3)	2022-09-26 (ds4)	Average accuracy（R^2）
Chl-a	R^2	0.91	0.92	0.89	0.91	0.91
	MRE(%)	14.62	13.17	14.93	14.81	14.38
	RMSE(mg/L)	3.76	3.58	4.01	3.89	3.81
TP	R^2	0.79	0.78	0.80	0.82	0.80
	MRE(%)	21.52	22.09	19.88	17.91	20.35
	RMSE(mg/L)	0.010	0.012	0.009	0.008	0.01
TN	R^2	0.83	0.81	0.81	0.79	0.81
	MRE(%)	18.39	19.25	19.08	21.48	19.55
	RMSE(mg/L)	0.051	0.062	0.059	0.079	0.06
COD_{Mn}	R^2	0.78	0.76	0.79	0.80	0.78
	MRE(%)	21.95	24.31	21.33	20.96	22.14
	RMSE(mg/L)	2.22	2.86	1.99	1.77	2.21

As shown in Table 1, the average inversion accuracy of water parameter Chl-a with obvious spectral response was relatively higher (the values of R^2, *MRE* and *RMSE* reach 0.91, 14.24% and 3.85mg/L respectively) than that of other three water quality parameters (TP, TN and COD_{Mn}) with weaker spectral response. The average inversion

International Water and Irrigation
ISSN: 0334-5807
Volume 44 Issue 2, (2025)
Pages 583-600

accuracies of TP, TN and COD_{Mn} were relatively lower, with R^2 values of 0.79, 0.82 and 0.78, *MRE* values of 21.16%, 18.31% and 22.53%, *RMSE* values of 0.010mg/L, 0.051mg/L and 2.36mg/L. According to the relevant industry standards or group standards in China such as the "*Technical guidelines for spectral on-line water quality monitoring system*"(T/CWEC 13-2019) , the spectral methods are considered effective for water quality monitoring if its mean relative error is less than 30%. Therefore, the inversion accuracies of the four water quality parameters (Chl-a, TP, TN and COD_{Mn}) in this work met the requirements of relevant industry or group standards. In order to more intuitively reflect the overall water quality of the reservoir from different perspectives, the concentration values and levels of water quality parameters can be used simultaneously to describe the spatial distribution of the overall water quality of the reservoir. This work classified the water quality of reservoirs according to the "*Environmental Quality Standards for Surface Water*" (GB 3838-2002 and GHZB1-1999).

Due to space limitations, in the following, only taking the water quality inversion results of WQR-DCRNN in Shanzai Reservoir on December 3, 2021 as an example. The inversion results of the four water quality parameters (Chl-a, TP, TN, and COD_{Mn}) are presented respectively (the inverted concentration values and corresponding national standard level distributions are shown in Figures 6-9), and the spatial distribution of eutrophication in Shanzai Reservoir on December 3, 2021 is comprehensively analyzed.

Chl-a is an important photosynthetic pigment in plant photosynthesis. By measuring the Chl-a concentration of phytoplankton, the junior productivity status and eutrophication level of water bodies can be analyzed. In environmental monitoring, Chl-a concentration can be used as one of the indexes of eutrophication in lakes. According to Figure 6, the distribution range of Chl-a concentration inversion values in Shanzai Reservoir, Fuzhou City on December 3, 2021 is 5.547~17.655 μ g/L. The overall water quality corresponds to levels III and IV of the standard values for lake and reservoir specific project in GHZB1-1999, and the spatial distribution of water quality is significantly different, that is, the Chl-a inversion concentration in the bottom-right branch of the reservoir is significantly lower than that in other parts. Except for the lower bottom-branch, mild eutrophication has occurred in other parts.

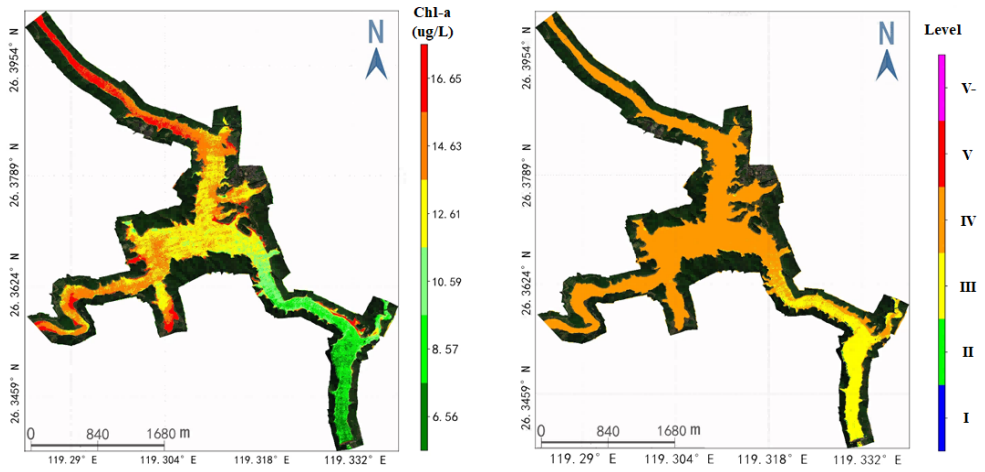

(a) (b)

Figure 6. Spatial distributions of Chl-a concentration inversion values (a) and corresponding national standard levels of China (b) in Shanzai Reservoir (2021-12-03).

Total phosphorus (TP) is the total content of phosphorus measured after the water sample is digested and various forms of phosphorus are converted into orthophosphates. Its main sources include domestic sewage, fertilizers, organic phosphorus pesticides, and phosphate cleaning agents. Phosphorus is one of the key elements required for the growth of algae in water bodies. Excessive phosphorus can cause water pollution and odor, eutrophication of

International Water and Irrigation
ISSN: 0334-5807
Volume 44 Issue 2, (2025)
Pages 583-600

lakes and reservoirs, and red tide in bays. According to Figure 7, the distribution range of TP concentration inversion values in the Shanzai Reservoir water body in Fuzhou City on December 3, 2021 is 0.007-0.037mg/L, and the spatial distribution difference is significant. The total TP concentration in the top-left branch is higher, and the overall water quality corresponds to levels I and II in GB3838-2002, with no obvious eutrophication phenomenon.

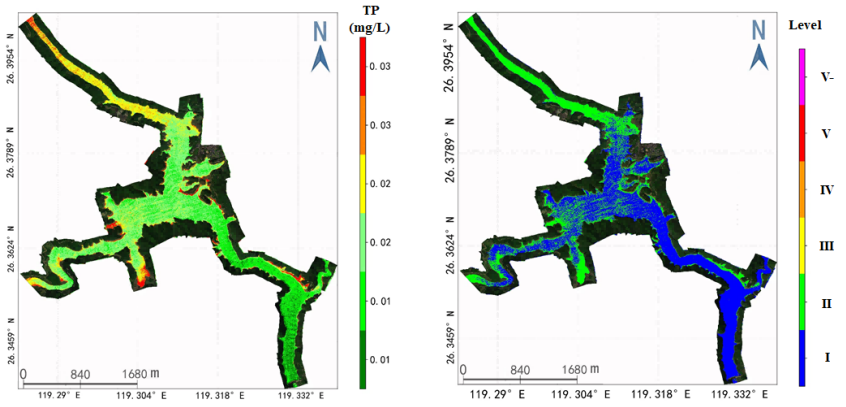

(a) (b)

Figure 7. Spatial distributions of TP concentration inversion values (a) and corresponding national standard levels of China (b) in Shanzai Reservoir (2021-12-03).

Total nitrogen (TN) refers to the total content of various forms of nitrogen in water, and is one of the important indexes for measuring the pollution and self-purification status of water bodies. Excessive nitrogen content in surface water can lead to the proliferation of microorganisms and vigorous growth of plankton, which may result in eutrophication of the water body. From Figure 8, it can be seen that the distribution range of TN concentration inversion values in the Shanzai Reservoir water body in Fuzhou City on December 3, 2021 is 0.048-1.228mg/L, with significant spatial distribution differences. The TN concentration in the bottom-right branch is generally lower, while the TN concentration of other parts of the reservoir is relatively higher. The water quality of the entire reservoir basically corresponds to levels II and III in GB3838-2002, and there is no obvious eutrophication phenomenon.

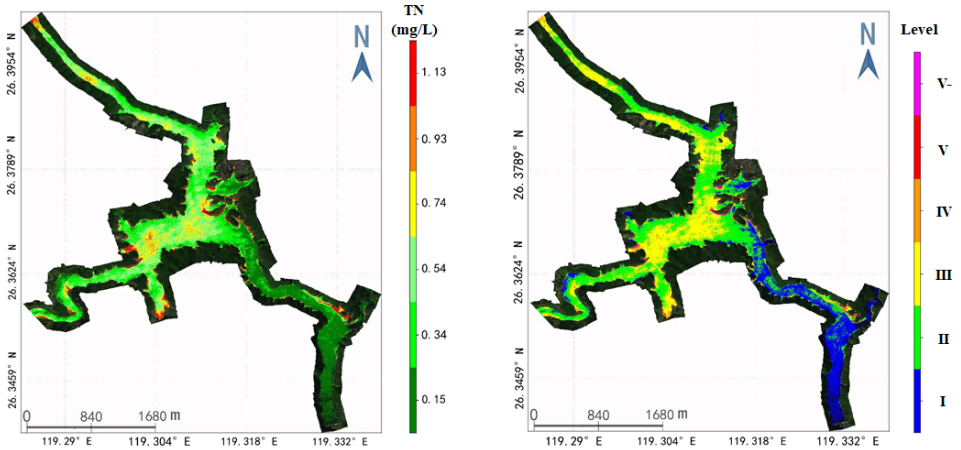

(a) (b)

Figure 8. Spatial distributions of TN concentration inversion values (a) and corresponding national standard levels of China (b) in Shanzai Reservoir (2021-12-03).

International Water and Irrigation
ISSN: 0334-5807
Volume 44 Issue 2, (2025)
Pages 583-600

Chemical Oxygen Demand (COD_{Mn}) is one of the commonly used indexes to measure the content of organic matters in water. The higher the COD_{Mn} value, the more severe the pollution of organic matters in surface water bodies. From the inversion results in Figures 9, it can be seen that distribution range of COD_{Mn} concentration inversion values in the Shanzai Reservoir water body in Fuzhou City on December 3, 2021 is 2.923~7.084mg/L, with significant spatial differences. The COD_{Mn} concentration in the central part of the reservoir is lower than that in the peripheral branches, and the overall water quality corresponds to level I in GB3838-2002, without obvious eutrophication phenomenon.

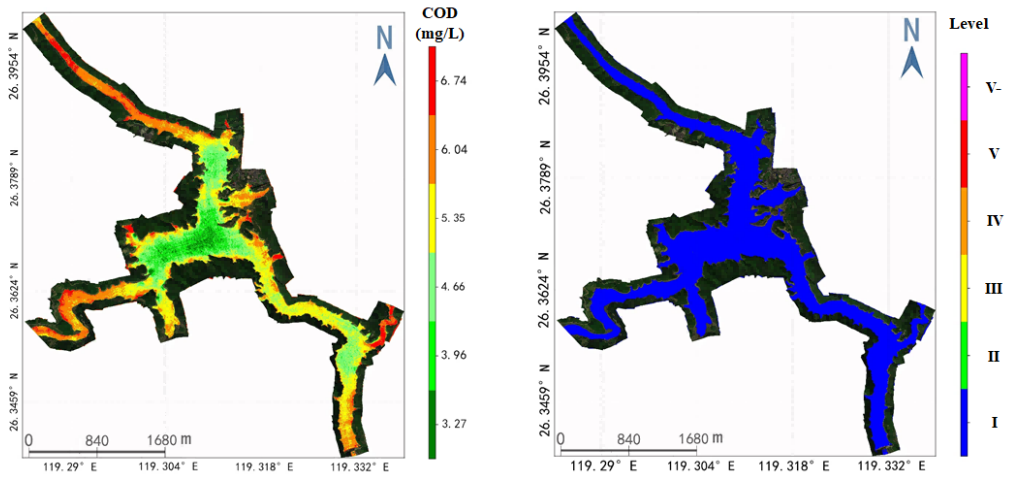

(a) (b)

Figure 9. Spatial distributions of COD_{Mn} concentration inversion values (a) and corresponding national standard levels of China (b) in Shanzai Reservoir (2021-12-03).

Overall, on December 3, 2021, the concentrations of TP, TN, and COD_{Mn} in the Shanzai Reservoir water in Fuzhou City were within the normal range, while the concentrations of Chl-a and TN were slightly higher, indicating mild eutrophication in the reservoir. Due to the lower winter temperatures, the growth of algae in the reservoir is somewhat inhibited, but factors such as construction around the reservoir or discharge of residential water may cause eutrophication of the reservoir water quality. In addition, by comprehensively analyzing the above water quality inversion results, the eutrophication status of Shanzai reservoir can be analyzed and preliminarily traced, the locations of sewage outlets along the reservoir can be analyzed, and the preliminary methods and policy recommendations for prevention and control of the eutrophication in the reservoir can be proposed.

The optimized WQR-DCRNN models can be directly embedded into airborne hyperspectral cameras, and the inversion results can be sent back to the ground through the image transmission mechanism and display on the screens of UAV remote controllers or ground control terminals, improving the real-time capabilities and practicality of water quality parameters inversion.

3.3 Comparative Experimental Analysis

Four algorithm models based on Random Forest (RF), Support Vector Machine Regression (SVR), K-Nearest Neighbor (KNN) and WQR-DCRNN were respectively used to invert the Chl-a, TP, TN and CODMn of Shanzai Reservoir waters in Fuzhou City at four different time phases: 2021-12-03, 2022-03-16, 2022-06-13 and 2022-09-26. The average accuracy of each algorithm model was compared, as shown in Table 2.

International Water and Irrigation
ISSN: 0334-5807
Volume 44 Issue 2, (2025)
Pages 583-600

Table 2. Analysis of Comparative Experimental Results.

Water quality parameter	Evaluation index	Average accuracy（R^2）			
		RF	SVM	KNN	WQR-DCRNN
Chl-a	R^2	0.81	0.79	0.68	0.91
	MRE(%)	18.04	20.11	29.16	14.24
	RMSE(mg/L)	4.59	6.18	10.92	3.85
TP	R^2	0.71	0.69	0.59	0.79
	MRE(%)	27.32	28.99	37.24	21.16
	RMSE(mg/L)	0.019	0.017	0.029	0.010
TN	R^2	0.73	0.71	0.62	0.82
	MRE(%)	25.18	27.25	34.61	18.31
	RMSE(mg/L)	0.081	0.092	0.131	0.051
CODMN	R^2	0.75	0.72	0.59	0.78
	MRE(%)	24.97	28.91	36.33	22.53
	RMSE(mg/L)	2.91	3.68	5.92	2.36

According to Table 2, due to deep learning algorithms have stronger capabilities of feature learning and non-linear complex function fitting, compared with the other three conventional machine learning algorithms, the WQR-DCRNN method proposed in this work has higher average accuracy, lower mean relative error and root mean square error for the inversion of four water quality parameters. The inversion accuracy of RF algorithm is only next to WQR-DCRNN, while the inversion accuracy of KNN algorithm is the lowest.

3.4. Performance Analysis of WQR-DCRNN Incremental Learning

The construction of the water quality concentration prediction models wd1~wd4 mentioned above is based on four sample sets ds1~ds4 (with 380, 372, 380 and 368 samples after augmentation respectively) in four different time phases, and the numbers of the training sample sets for each model construction are relatively limited. Due to the high demand for the number of training samples in deep learning models, increasing the number of training samples can improve the accuracy and robustness of the WQR-DCRNN model to some extent. In addition, with the increase of sampling times, the number of relevant samples will also continue to increase. The old WQR-DCRNN model constructed from the original sample set needs to be constantly updated and iterated. Good incremental learning ability can effectively preserve the key features of the old WQR-DCRNN model, thereby avoiding repeated training on the old sample set and improving the efficiency of WQR-DCRNN model update and iteration.

This work gradually increased the number of training samples for the WQR-DCRNN models construction in four stages by accumulating four temporal samples sets one by one. The sample sets for stages 1 to 4 were ds1, ds1+ds2, ds1+ds2+ds3, and ds1+ds2+ds3+ds4, respectively. The WQR-DCRNN models in the four stages were constructed as w1, w12, w123 and w1234, and the above models were optimized to improve their generalization and incremental learning abilities. We conducted inversion experiments on four water quality parameters (Chl-a, TP, TN and CODMn) using models w1, w12, w123, and w1234 respectively. The results are shown in Table 3.

International Water and Irrigation
ISSN: 0334-5807
Volume 44 Issue 2, (2025)
Pages 583-600

Table 3. Incremental Learning Results of WQR-DCRNN.

Water quality parameter	Evaluation index	Average accuracy（R^2）			
		2021-12-03 (w1)	2022-03-16 (w12)	2022-06-13 (w123)	2022-09-26 (w1234)
Chl-a	R^2	0.91	0.88	0.89	0.93
	MRE(%)	14.62	15.63	15.34	12.71
	RMSE(mg/L)	3.76	4.39	4.11	3.36
TP	R^2	0.79	0.78	0.81	0.83
	MRE(%)	21.52	22.18	19.57	17.44
	RMSE(mg/L)	0.010	0.012	0.008	0.006
TN	R^2	0.83	0.81	0.83	0.85
	MRE(%)	18.39	19.05	18.34	15.52
	RMSE(mg/L)	0.051	0.061	0.050	0.046
CODMN	R^2	0.78	0.77	0.79	0.80
	MRE(%)	21.95	24.19	21.36	20.77
	RMSE(mg/L)	2.22	2.78	1.97	1.72

According to Table 3, the WQR-DCRNN model has good incremental learning ability and robustness. The w1, w12, w123, and w1234 models were used to invert the four water quality parameters (Chl-a, TP, TN and CODMn) in Shanzai Reservoir with overall high and stable accuracy. Especially, w1234 has significantly improved the inversion accuracy of Chl-a, TP and TN, while the inversion accuracy of CODMn remains basically stable.

4. Discussion

Although compared with conventional machine learning algorithms (such as RF, SVR and KNN), the WQR-DCRNN model proposed in this work has higher accuracy in water quality inversion. However, WQR-DCRNN also has some shortcomings (such as more training sample requirements and longer training time consumption) due to the use of deep learning models with more complex network structures. Carrying out large-scale reservoir eutrophication inversion requires more computing power and storage capacity support. Due to regional limitations, seasonal changes and human activities, the construction of reservoir water quality inversion models is a long-term project that requires accumulation and updating. Although WQR-DCRNN has good incremental learning ability, its versatility and scalability in the inversion of eutrophication in different reservoir water bodies still needs further verification.

In addition, there is no unified standard framework for evaluating the eutrophication status of reservoirs both domestically and internationally currently. The commonly used indexes for evaluating the eutrophication status of inland reservoirs can be divided into two categories: comprehensive indexes and single water quality indexes. The former generally includes Trophic State Index (TSI), Trophic Level Index (TLI), Forel Ule Index (FUI), Probability of Eutrophication Occurrence (PEO), etc. The latter mainly includes the six indexes of Chl-a ,COD_{Mn},TN,TP, TSS and SD (Secchi Disk Depth, that is, transparency). The comprehensive indexes (such as

International Water and Irrigation
ISSN: 0334-5807
Volume 44 Issue 2, (2025)
Pages 583-600

TSI and TLI) are generally continuous grading methods of eutrophication status for lakes and reservoirs based on the sensitivity of a single benchmark factor and multiple auxiliary factors. The above factors are combined by weighting, and the weight allocation has a certain subjectivity, which is more suitable for evaluating the eutrophication status of large lakes and reservoirs. For small and medium-sized lakes and reservoirs, single water quality indicators are generally used for evaluation, and the data sources are mainly medium to high-resolution aerial images (including UAV images) [18-20]; The concentrations of Chl-a, TP, TN and COD_{Mn} can effectively reflect the growth status of phytoplankton and algae in water bodies, as well as the pollution of organic matters in water bodies. They are currently mature representative indicators for measuring the degree of eutrophication in lake and reservoir water bodies. Therefore, this study adopts four water quality parameters, Chl-a, TP, TN, and CODMn, as evaluation indicators for eutrophication in Shanzai Reservoir (a small and medium-sized reservoir) in Fuzhou City, which has strong rationality.

5. Conclusions

This work proposes a reservoir water quality parameter inversion scheme based on deep learning and UAV hyperspectral remote sensing images to address the problem of insufficient accuracy in remote sensing inversion of eutrophication in large-scale reservoirs. Taking Shanzai Reservoir in Fuzhou City as an example, four water quality parameters (Chl-a, TP, TN and CODMn) are used as the evaluation indexes for eutrophication in the reservoir. For each of the above water quality parameters, corresponding WQR-DCRNN models were trained and constructed using four different temporal sample sets. Then different temporal WQR-DCRNN models were used to invert the water quality parameters of the reservoir at the corresponding time phase. The spatial distribution maps of concentration values and corresponding national standard levels of the four different water quality parameters at four different time phases were obtained, and the average inversion accuracy (R^2) of the four different water quality parameters reached 0.91, 0.80, 0.81 and 0.78, respectively. Compared with machine learning methods such as RF, SVR and KNN, WQR-DCRNN achieved higher water inversion accuracy, and the mean relative error (MRE) was better than that in relevant industry or group standard requirements of water quality spectral monitoring method. In addition, by gradually training and updating the WQR-DCRNN model through the accumulation of multiple temporal sample sets, the final inversion accuracies of the four water quality parameters reached 0.93, 0.83, 0.85 and 0.80, respectively, indicating that WQR-DCRNN has higher prediction accuracy, stability and incremental learning ability than RF, SVR and KNN. Of course, compared with traditional noodle learning methods, WQR-DCRNN also has problems such as more training sample requirements and longer training time consumption due to the use of deep learning models with more complex network structures. In summary, large-scale dynamic monitoring of eutrophication status in reservoir water quality can be performed by WQR-DCRNN, so as to improve the accuracy and practicality of remote sensing inversion of reservoir water quality, and provide useful references for the assessment and prevention of eutrophication in reservoir water quality.

Author Contributions: Conceptualization, F.H.; methodology, F.H. and B.L.; validation, Y.L. and Z.Y.Z.; formal analysis, F.H., B.L. and Z.Z.; investigation, Y.L., Z.Y.Z. and Z.Z.; data curation, Y.L., Z.Z. and J.L.; writing—original draft preparation, F.H.and B.L.; writing—review and editing, F.H., Y.L. and Z.Z.;supervision, F.H., Z.Z.and J.L.; funding acquisition, F.H.. All authors have read and agreed to the published version of the manuscript.

Funding: This research was funded by the National Natural Science Foundation of China (NSFC, 41501451), China Postdoctoral Science Foundation (2015M571963), Open Fund Project of Fujian Key Laboratory of Spatial Information Perception and Intelligent Processing (FKLSIP1015),Fujian Province Young and Middle aged Teacher Education Research Project (JZ240084).

Data Availability Statement: The datasets presented in this article are not readily available because some data is confidential. Requests to access these datasets should be directed to the Fujian Key Laboratory of Spatial Information Perception and

International Water and Irrigation
ISSN: 0334-5807
Volume 44 Issue 2, (2025)
Pages 583-600

Intelligent Processing (Yango University) in China.

Acknowledgments: The authors would like to thank Jun Cao and Ying Yu in College of Artificial Intelligence (China) for their assistance, suggestions, and discussions.

Conflicts of Interest: The authors declare no conflict of interest.

References

[1] Xiang P. Academician Chenghu Zhou: Water Conservancy Applications of Remote Sensing Big Data. High-Technology and Industrialization 2023, 330:12-15.
[2] Nanjing Institute of Geography and Limnology, Chinese Academy of Sciences. Chinese Lake Survey Report; Science Press: Beijing, China, 2019 ; pp. 5-20.
[3] Zhou B.T.; Zhang Y. Y.; Shi K. Research progress on remote sensing assessment of lake nutrient status and retrieval algorithms of characteristic parameters. Journal of Remote Sensing 2022, 26: 77-91.
[4] Wang S. M.; Qin B.Q. Research progress on remote sensing monitoring of lake water quality parameters. Environmental Science 2023, 44: 1228-1243.
[5] Zhang L. P.; Zhang L. F.; Yuan Q. Q. Large remote sensing model: progress and prospects. Geomatics and Information Science of Wuhan University 2023, 48: 1574-1581.
[6] Wang B.; Huang J. H.; Guo H. W.; et al. Progress in research on inland water quality monitoring based on remote sensing. Water Resources Protection 2022, 38:117-124.
[7] Wang X. Y.; Yang W. Water quality monitoring and evaluation using remote sensing techniques in China: a systematic review. Ecosystem Health & Sustainability 2019, 5: 47-56.
[8] Wang S. L.; Li J. S.; Zhang B.; et al. Changes of water clarity in large lakes and reservoirs across China observed from long-term MODIS. Remote Sensing of Environment 2020, 247: 111949-111965.
[9] Saberioon M.; Brom J.; Nedbal V.,et al. Chlorophyll-a and total suspended solids retrieving and mapping using Sentinel-2 and machine learning for inland waters. Ecological Indicators 2020, 113:106236-106257.
[10] Chen C.; Chen Q. W.; Li G.; et al. A novel multi-source data fusion method based on Bayesian inference for accurate estimation of chlorophyll-a concentration over eutrophic lakes. Environmental Modelling and Software 2021, (141):105057-105068.
[11] Cao Z. G.; Ma R. H.; Duan H. T.; et al. A machine learning approach to estimate chlorophyll-a from Landsat-8 measurements in inland lakes. Remote Sensing of Environment 2020, 248: 111974-111988.
[12] Guo H. W.;Huang J. J.; Chen B. W.; et al. A machine learning-based strategy for estimating non-optically active water quality parameters using Sentinel-2 imagery. International Journal of Remote Sensing 2021, 42: 1841-1866.
[13] Feng C. J.; Fang C. Q.; Yuan G. Y.; et al. Water pollution monitoring based on unmanned aerial vehicle (UAV) hyperspectral and BP neural network. Chinese Journal of Environmental Engineering 2023, 17: 3996-4006.
[14] Sheng H.; Chi H. X.; Xu M. M.; etc. Inland water chemical oxygen demand estimation based on improved SVR for hyperspectral Data. Spectroscopy and spectral analysis 2021, 41: 3565-3571.
[15] Zhang Y.S.; Wu L.; Ren H.Z.; et al. Retrieval of water quality parameters from hyperspectral images using hybrid Bayesian probabilistic neural network. Remote Sensing 2020, 12: 1567-1597.
[16] Wan H.;Xu R.; Zhang M.;et.al. A novel model for water quality prediction caused by non-point sources pollution based on deep learning and feature extraction methods. Journal of Hydrology 2022, 612:128081-128091.
[17] Niu C.; Tan K.; Jia X. P.;Wang X.Deep learning based regression for optically inactive inland water quality parameter estimation using airborne hyperspectral imagery. Environmental Pollution 2021, 286:117534-117558.

International Water and Irrigation
ISSN: 0334-5807
Volume 44 Issue 2, (2025)
Pages 583-600

[18] Wu Y.; Deng R.R.; Qin Y.;Liang Y.H.; Xiong L.H. The Study of Spatial-Temporal Characteristics for Chlorophyll Concentration derived from Remote Sensing Image in Xinfengjiang Reservoir. Remote Sensing Technology and Application 2017, 32:825-834.
[19] Ogashawara I.;Mishra D.;Gitelson A. Remote sensing of inland waters: Background and current state-of-the-Art. Bio-optical Modeling and Remote Sensing of Inland Waters; Elsevier:Amsterdam,Netherlands, 2017;pp.1-24.
[20] Li J.;Yu Q.;Tian Y.; et al. Spatio-temporal variations of CDOM in shallow inland waters from a semianalytical inversion of Landsat-8. Remote Sensing of Environment 2018, 218: 189-200.